Calpain 12 Function Revealed through the Study of an Atypical Case of Autosomal Recessive Congenital Ichthyosis

Ron Bochner[1,12], Liat Samuelov[1,2,12], Ofer Sarig[1,12], Qiaoli Li[3], Christopher A. Adase[2], Ofer Isakov[4,5], Natalia Malchin[1], Dan Vodo[1,6], Ronna Shayevitch[6], Alon Peled[1,6], Benjamin D. Yu[2], Gilad Fainberg[1], Emily Warshauer[1], Noam Adir[7], Noam Erez[8], Andrea Gat[9], Yehonatan Gottlieb[10], Tova Rogers[1], Mor Pavlovsky[1], Ilan Goldberg[1], Noam Shomron[4,5], Aileen Sandilands[11], Linda E. Campbell[11], Stephanie MacCallum[11], W. H. Irwin McLean[11], Gil Ast[6], Richard L. Gallo[2], Jouni Uitto[3] and Eli Sprecher[1,6]

Congenital erythroderma is a rare and often life-threatening condition, which has been shown to result from mutations in several genes encoding important components of the epidermal differentiation program. Using whole exome sequencing, we identified in a child with congenital exfoliative erythroderma, hypotrichosis, severe nail dystrophy and failure to thrive, two heterozygous mutations in *ABCA12* (c.2956C>T, p.R986W; c.5778+2T>C, p. G1900Mfs*16), a gene known to be associated with two forms of ichthyosis, autosomal recessive congenital ichthyosis, and harlequin ichthyosis. Because the patient displayed an atypical phenotype, including severe hair and nail manifestations, we scrutinized the exome sequencing data for additional potentially deleterious genetic variations in genes of relevance to the cornification process. Two mutations were identified in *CAPN12*, encoding a member of the calpain proteases: a paternal missense mutation (c.1511C>A; p.P504Q) and a maternal deletion due to activation of a cryptic splice site in exon 9 of the gene (c.1090_1129del; p.Val364Lysfs*11). The calpain 12 protein was found to be expressed in both the epidermis and hair follicle of normal skin, but its expression was dramatically reduced in the patient's skin. The downregulation of capn12 expression in zebrafish was associated with abnormal epidermal morphogenesis. Small interfering RNA knockdown of *CAPN12* in three-dimensional human skin models was associated with acanthosis, disorganized epidermal architecture, and downregulation of several differentiation markers, including filaggrin. Accordingly, filaggrin expression was almost absent in the patient skin. Using ex vivo live imaging, small interfering RNA knockdown of calpain 12 in skin from *K14-H2B GFP* mice led to significant hair follicle catagen transformation compared with controls. In summary, our results indicate that calpain 12 plays an essential role during epidermal ontogenesis and normal hair follicle cycling and that its absence may aggravate the clinical manifestations of *ABCA12* mutations.

Journal of Investigative Dermatology (2017) **137,** 385–393; doi:10.1016/j.jid.2016.07.043

INTRODUCTION

Congenital erythroderma refers to a genetically and phenotypically heterogeneous group of disorders of cornification featuring generalized redness and scaling present at birth (Pruszkowski et al., 2000). Although congenital erythroderma has been associated with a number of acquired and hereditary disorders, the vast majority of cases are due to inherited mutations in genes encoding important components of the epidermal differentiation program. Among the various etiologies associated with congenital erythroderma, autosomal recessive congenital ichthyoses (ARCIs) rank first (Pruszkowski et al., 2000). ARCIs are caused by mutations in genes encoding proteins involved in the formation of the epidermal barrier, such as *ABCA12*, encoding a transporter

[1]*Department of Dermatology, Tel Aviv Sourasky Medical Center, Tel Aviv, Israel;* [2]*Department of Dermatology, University of California, San Diego, California, USA;* [3]*Department of Dermatology and Cutaneous Biology, Sidney Kimmel Medical College at Thomas Jefferson University, Philadelphia, Pennsylvania, USA;* [4]*Department of Cell and Developmental Biology, Sackler Faculty of Medicine, Tel Aviv University, Tel Aviv, Israel;* [5]*Variantyx Ltd, Ashland, USA;* [6]*Department of Human Molecular Genetics and Biochemistry, Sackler Faculty of Medicine, Tel Aviv University, Tel Aviv, Israel;* [7]*Schulich Faculty of Chemistry, Technion-Israel Institute of Technology, Haifa, Israel;* [8]*The Research Center for Digestive Tract and Liver Diseases, Tel Aviv Sourasky Medical Center, Tel Aviv, Israel;* [9]*Department of Pathology, Tel Aviv Sourasky Medical Center, Tel Aviv, Israel;* [10]*Research Laboratory for Pediatric Hemato-Oncology, Dana Children's Hospital, Tel Aviv Sourasky Medical Center, Tel Aviv, Israel; and* [11]*Centre for Dermatology and Genetic Medicine, Division of Biological Chemistry and Drug Discovery, School of Life Sciences, University of Dundee, Dundee, UK*

[12]*These authors contributed equally to this work.*

Correspondence: Eli Sprecher, Department of Dermatology, Tel Aviv Sourasky Medical Center, 6, Weizmann Street, Tel Aviv 64239, Israel. E-mail: elisp@tlvmc.gov.il

Abbreviations: ARCI, autosomal recessive congenital ichthyose; PCR-RFLP, PCR-restriction fragment length polymorphism; siRNA, small interfering RNA

Received 28 March 2016; revised 14 June 2016; accepted 18 July 2016; accepted manuscript published online 18 October 2016; corrected proof published online 9 December 2016

involved in lipid loading within epidermal lamellar granules (Oji et al., 2010).

Congenital erythroderma is not only characterized by extensive genetic heterogeneity, but it is also characterized by striking clinical variability, which has suggested the existence of modifying genetic variants responsible for aggravating or attenuating disease phenotypes (Cooper et al., 2013). The identification of modifier variants can sometimes reveal important biological functions. In this study, the delineation of the molecular basis of an atypical case of congenital erythroderma revealed a hitherto unknown role for calpain 12 (CAPN12) during epidermal differentiation and hair follicle cycling.

RESULTS

Phenotype delineation

A 6-week-old boy was referred for investigation because of congenital erythroderma and failure to thrive. The patient was the second child of healthy unrelated parents of Palestinian Armenian and Palestinian Catholic origin. He had a healthy brother and there was no family history of skin or hereditary diseases. The patient was born after 34 weeks of gestation. At birth, his skin was reddish and partly covered with thick grayish secretions, but his hair was normal. He was hospitalized in the pediatric intensive care unit, where he was treated with intravenous antibiotics during three episodes of sepsis associated with hypoglycemia and hypocalcemia. Over the first 2 weeks of life, the skin became red and scaly (Figure 1a), and he progressively lost most of his hair. General and neurological examinations were normal. Apart from ectropion, ophthalmological examination was normal. Complete blood count, blood chemistry, and IgE levels were normal. Blood smear was normal with no evidence of Jordan's anomaly. Ultrasound examination of the abdomen and pelvis was unrevealing. Repeated echocardiograms and the Brainstem Evoked Response Audiometry (*BERA*) hearing test were normal.

Over the first 2 years of life, the patient failed to grow (currently below the third percentile) but did not experience any additional infectious complications. Although his skin condition remained stable and some hair growth was noticed (Figure 1b), massive overgrowth of his nail plates (Figure 1c) became evident at the age of 1 year, markedly interfering with daily function.

A skin biopsy revealed a perivascular, psoriasiform dermatitis with parakeratosis, and a relatively thin stratum corneum showing intracorneal splitting (Figure 1d). Hair microscopy was unremarkable (not shown).

Mutation analysis

Because the patient's clinical features (congenital erythroderma, skin peeling, hypotrichosis) were reminiscent of Netherton syndrome or related syndromes (Samuelov and Sprecher, 2014), we initially excluded mutations in *SPINK5*, *CDSN*, and *DSG1* by direct sequencing (not shown). A DNA sample from the patient was then subjected to whole exome sequencing and data were initially scrutinized for mutations in genes known to be associated with disorders of cornification (Oji et al., 2010), leading to the identification of two heterozygous mutations in *ABCA12* (Figure 2a): c.2956C>T, predicted to result in p.R986W substitution, and c.5778+2T>C, predicted to abolish a conserved donor splice site located in intron 38 and to result in p. G1900Mfs*16. Despite the fact that only one of the two mutations (p.R986W) has been published previously (Fukuda et al., 2012), a number of facts support the possibility that they are pathogenic. Both mutations were found to cosegregate with the disease phenotype (Figure 2b). Mutation c.2956C>T was found in 3 of 134,322 alleles deposited in public databases including NCBI, HGMD, UCSC, ENSEMBL, 1000 Genomes Project, ExAc, and the NHLBI Grand Opportunity Exome Sequencing Project, whereas mutation c.5778+2T>C was not found in any of the public databases mentioned above. Both mutations were excluded using PCR-restriction fragment length polymorphism (PCR-RFLP) assays from a cohort of 274 and 207 population-matched nonaffected individuals, respectively. Mutation p.R986W affects a highly conserved residue (Conseq = 9, range 1–9; http://conseq.tau.ac.il/) and is predicted to be damaging by PolyPhen-2 (score = 1; http://genetics.bwh.harvard.edu/pph2/) and SIFT (score = 0; http://sift.jcvi.org/) software. To assess the consequences of mutation c.5778+2T>C, we sequenced cDNA derived from a patient skin biopsy with a primer pair encompassing exons 37–39. As shown in Figure 2c, the

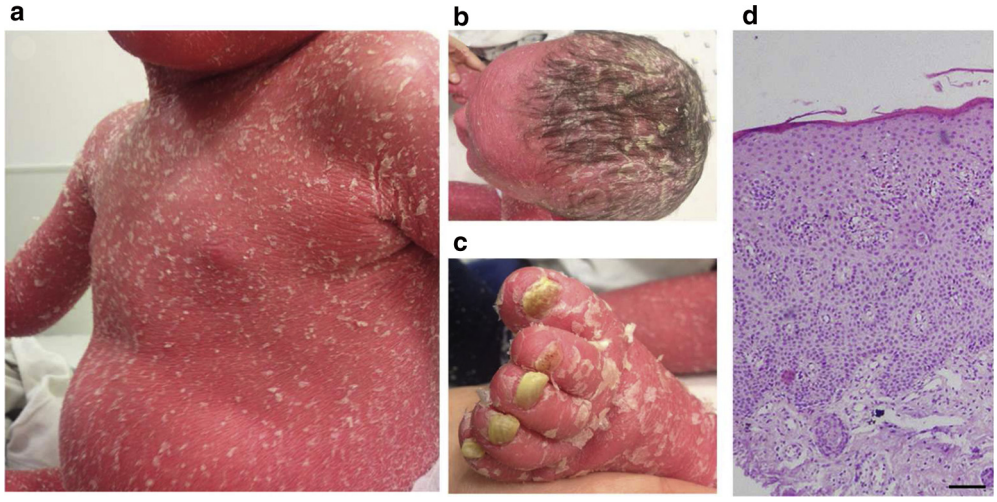

Figure 1. Clinical and pathological features. The proband demonstrates (**a**) exfoliative erythroderma, (**b**) hypotrichosis and thick yellowish scales over the scalp, and (**c**) hypertrophic nails. (**d**) On histology, parakeratosis, acanthosis, and mild perivascular dermatitis are seen (hematoxylin and eosin; scale bar = 100 μm).

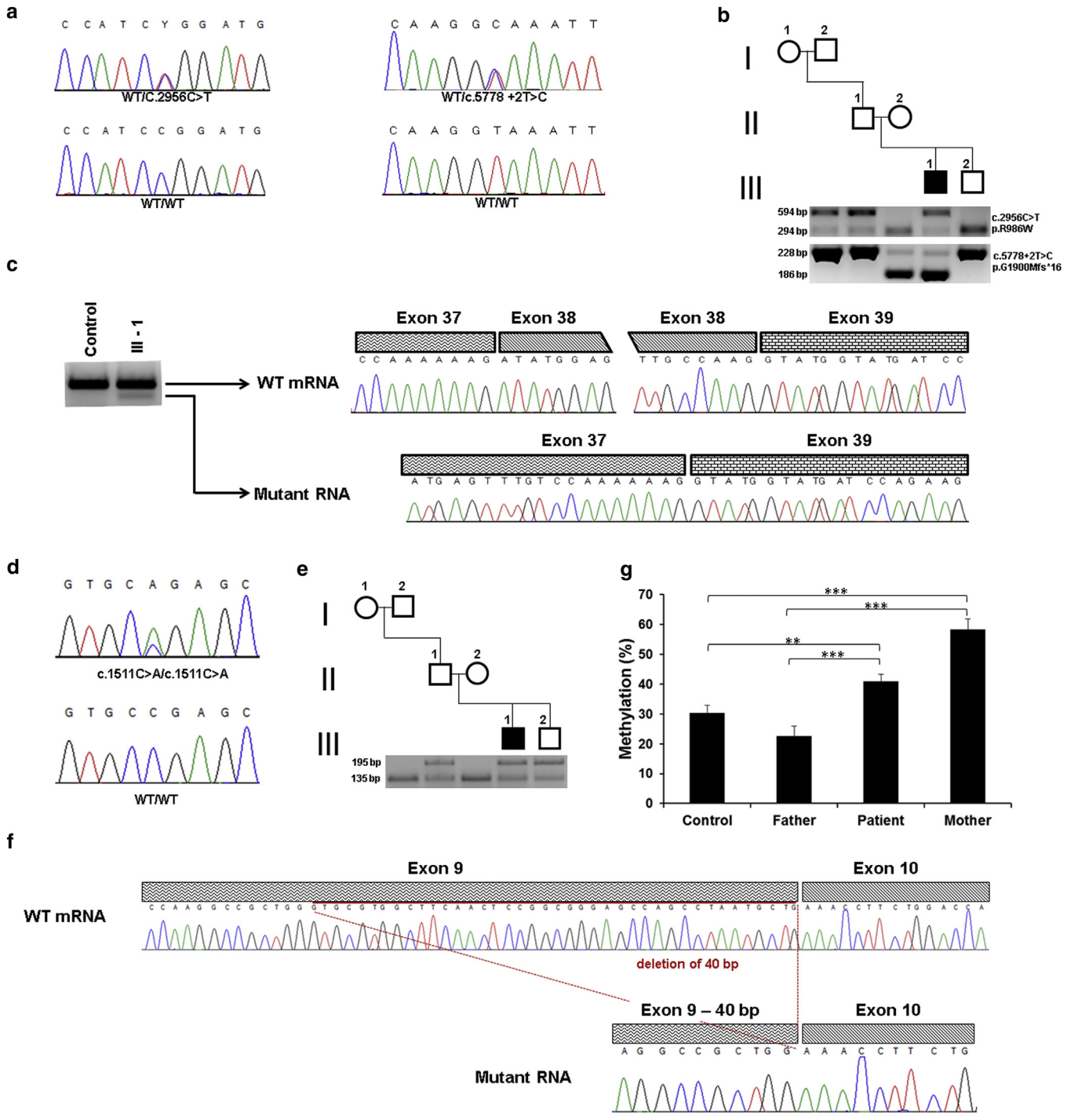

Figure 2. Mutation analysis. (**a**) Direct sequencing of *ABCA12* revealed two heterozygous mutations: a C>T transition at position c.2956 of the DNA sequence (upper-left panel) and a T>C transition at position c.5778+2 (upper-right panel). The wild-type (WT) sequences are given for comparison (lower panels). (**b**) A PCR-restriction fragment length polymorphism (RFLP) assay was used to assess cosegregation of the two *ABCA12* mutations with the disease phenotype. The c.2956C>T and c.5778+2T>C mutations are associated with the presence of 594-bp and 186-bp fragments, respectively. (**c**) cDNA was reverse transcribed from RNA extracted from the skin of the patient and of a healthy individual (WT). cDNA was PCR amplified using primers spanning *ABCA12* exons 37–39 (left panel). Direct sequencing of the resulting amplicons revealed a WT mRNA sequence in both the patient and the healthy individual (upper-right panel) as well as a shorter isoform due to exon 38 skipping, in the patient only (lower-right panel). (**d**) Direct sequencing of *CAPN12* revealed a heterozygous C>A transversion at position c.1511 of the cDNA sequence (upper panel). The WT sequence is given for comparison. (**e**) A PCR-RFLP assay was used to assess cosegregation of the c.1511C>A mutation in *CAPN12* with the disease phenotype. The mutation is associated with the presence of a 195-bp fragment. (**f**) cDNA was reverse transcribed from RNA extracted from the skin of the patient and PCR amplified using primers spanning *CAPN12* exon 8–10. Direct sequencing of the resulting amplicons revealed WT mRNA sequence (upper panel) as well as a shorter sequence lacking the last 40 bp of exon 9 (lower panel). (**g**) DNA methylation analysis of *CAPN12* exon 9 was performed using DNA extracted from keratinocytes derived from skin biopsies of the patient, his mother, and father as well as two unrelated control individuals. For details, see Supplementary Materials and Methods. Results represent the mean results derived from the analysis of 10–15 clones per sample ± SE (**$P < 0.05$; ***$P < 0.01$, two-sided *t*-test).

mutation was found to result in an 88-bp deletion, due to exon 38 skipping, which in turn is likely to result in mRNA decay as demonstrated in Figure 2c.

As mentioned above, *ABCA12* mutations have been shown to cause both ARCI and harlequin ichthyosis. Our patient clearly did not display a phenotype resembling harlequin ichthyosis, and hypotrichosis with exuberant nail growth is not typical of ARCI.

We therefore reascertained the whole exome sequencing data for additional deleterious sequence alterations of potential relevance to the skin phenotype displayed by the patient. We looked for rare and functionally relevant changes and therefore applied the following filtration criteria (Isakov et al., 2013a, 2013b): *Minor allele* frequency (MAF) < 0.01 (and no more than 25 carriers reported); high conservation as predicted by four bioinformatics software packages: Conseq (Berezin et al., 2004) > 8, Phylop (Siepel et al., 2006) > 0.85, GERP (Pollard et al., 2010) > 1.5, and phast-Cons-Elements-46way (Siepel et al., 2005); and deleterious effects on protein function as predicted by PolyPhen2 (Adzhubei et al., 2010) > 0.95 and SIFT (Kumar et al., 2009) < 0.05. Only one heterozygous transversion, c.1511C>A in *CAPN12*, passed all functional filters and is predicted to result in p.P504Q substitution.

CAPN12 encodes calpain 12, a calcium-activated cysteine protease, which belongs to a group of proteins that have been shown to play an important role in epidermal differentiation (Campbell and Davies, 2012; Ono and Sorimachi, 2012) and have recently been implicated in the pathogenesis of a human skin disease (Lin et al., 2015). *Capn12* was shown in mice to be exclusively expressed in the skin (Dear et al., 2000). Accordingly, we found out that it is mainly expressed in human skin with weaker to almost absent expression in other tissues (Supplementary Figure S1 online).

The mutation was identified by direct sequencing (Figure 2d) and a PCR-RFLP assay (Figure 2e) in the patient, his father, and his brother, but not in the patient's mother. The mutation was found in 2 of 25,126 alleles deposited in public databases including NCBI, HGMD, UCSC, ENSEMBL, 1000 Genomes Project, ExAc, and the NHLBI Grand Opportunity Exome Sequencing Project. Using the PCR-RFLP assay described above, we excluded the mutation from a panel of 176 population-matched healthy controls. The mutation affects a highly conserved amino acid residue (Conseq = 9, range 1−9) and is likely to be damaging to the protein function (SIFT score = 0, PolyPhen-2 score = 0.997). The sequence of CAPN12 (NP_653292.2) was submitted to the Phyre2 Protein Fold recognition server (https://www.ncbi.nlm.nih.gov/gene/?term=NP_653292.2) to obtain a molecular model. A large number of Calpain and Calpain-like structures have been experimentally determined and deposited in the Protein Data Bank (http://www.rcsb.org/pdb/home/home.do). CAPN12 was modeled according to the human m-calpain large subunit structure (PDB code 1KFX:L) with a statistical confidence of 100% (residues 1−719). The site of the mutation P504 is located within the central domain of the protein, which includes a large β-sandwich motif (Supplementary Figure S2 online). This domain is surrounded by the N-terminal and C-terminal domains and likely stabilizes the entire protein fold. The proline pyrrolidine side chain faces into the sandwich interface directly facing and participating in a highly hydrophobic core that includes W363, F359, and F385. Mutation of the polar and bulky glutamine residue is predicted to have a disrupting effect on this hydrophobic core, destabilizing the sandwich interactions.

Full sequencing of the entire coding and noncoding (including the promoter region) sequence of *CAPN12* in the proband and his mother failed to reveal a second pathogenic sequence alteration. However, direct sequencing of a cDNA sample derived from a skin biopsy obtained from the patient revealed a 40-bp deletion, presumably due to activation of a cryptic splice site within exon 9 of the gene (Figure 2f). The heterozygous mutation c.1090_1129del is predicted to result in frameshift, premature protein termination (p.Val364-Lysfs*11), and most likely, nonsense-mediated mRNA decay. To confirm segregation of the mutation with the disease phenotype, we obtained skin biopsies from the patient's parents. Using direct sequencing of biopsy-derived cDNA, we demonstrated the presence of the c.1090_1129del mutation in the cDNA generated from the patient's mother, but not in the cDNA generated from the patient's father (not shown).

Because we failed to identify any DNA or RNA sequence alteration that could have caused activation of the cryptic splice site in exon 9 of the *CAPN12* gene, we hypothesized that epigenetic changes may possibly underlie this phenomenon. Indeed, a steadily growing body of evidence suggests that exonic DNA methylation is associated with increased alternative splicing (Lev Maor et al., 2015; Malousi and Kouidou, 2012; Maunakea et al., 2013). We therefore compared the DNA methylation pattern in the patient, his parents, and control individuals. Both the patient and his mother demonstrated significantly increased DNA methylation in exon 9 (Figure 2g) as compared with all other DNA samples. Of interest, these differences in methylation status were noticed in keratinocytes but not in peripheral blood lymphocytes (not shown), suggesting that hypermethylation-associated alternative splicing within *CAPN12* may be tissue specific, as previously shown for other genes (Gutierrez-Arcelus et al., 2015). To assess the functional consequences of the presence of the two deleterious *CAPN12* mutations that were identified in the patient, we compared the pattern of expression of calpain 12 in the skin of the patient and in normal skin. As shown in Figure 3a, calpain 12 is strongly expressed in normal epidermis, as previously shown in murine skin, but was absent in the patient skin. Using quantitative real-time reverse transcriptase-PCR, we found out that *CAPN12* RNA levels were eightfold lower in the patient skin as compared with normal skin (Figure 3b).

Delineation of CAPN12 function in the epidermis

Little is currently known about the function of calpain 12 in the epidermis (Dear et al., 2000). Over the past few years, the zebrafish has become recognized as a useful model to ascertain the importance of mediators of human epidermal development (Li and Uitto, 2013). We therefore downregulated the expression of *capn12* in zebrafish using a gene-specific morpholino (Supplementary Figure S3 online). Scanning electron microscopy of morphant larvae at 3 dpf revealed abnormally large keratinocytes with aberrant microridge formation as compared with normal keratinocytes in control larvae

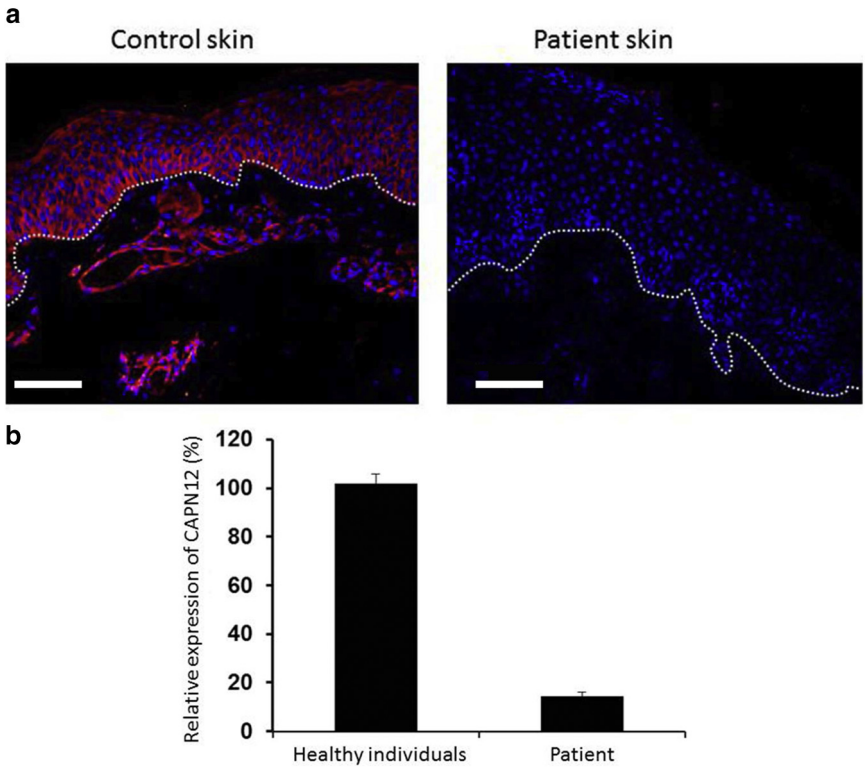

Figure 3. CAPN12 expression in the skin. (**a**) A skin biopsy obtained from a healthy individual demonstrates by immunostaining cytoplasmic expression of calpain 12 in the epidermis (more pronounced in the lower epidermal layers) (left panel). In contrast, calpain 12 expression is markedly reduced in the skin of the patient (right panel) (dermoepidermal junction is marked with a dotted line; scale bars = 100 μm). (**b**) Quantitative real-time reverse transcriptase-PCR analysis was used to assess *CAPN12* RNA expression in cDNA samples derived from healthy individual skin and patient skin. Results represent the mean of three replicates and are provided as percentage of expression relative to gene expression in four controls ± SE normalized to *ACTB* mRNA levels.

(Figure 4a and b). In addition, transmission electron microscopy analysis demonstrated almost complete absence of microridges in the morphant larvae (Figure 4c and d) that also developed pericardial edema and curled tail phenotype (Figure 4e and f), associated with death at 6–8 dpf.

We then used two in vitro models to determine whether calpain 12 is involved in epidermal differentiation and hair cycling. First, using small interfering RNA (siRNA), we downregulated *CAPN12* expression in primary keratinocytes and used these keratinocytes to generate three-dimensional skin equivalents (Supplementary Figure S4 online). As shown in Figure 5a and Supplementary Figure S5 online, *CAPN12* downregulation resulted in a disorganized epidermal architecture associated with mild acanthosis, suggesting abnormal differentiation. Keratin gene expression was also consistent with abnormal epidermal differentiation (Supplementary Figure 6S online). We therefore analyzed the pattern of expression of filaggrin, which has been shown to be a substrate of calpains[38] and is a marker of terminal differentiation in the epidermis. Filaggrin was almost absent and mislocalized in organotypic skin equivalents downregulated for *CAPN12*, as well as in the skin of the patient (Figure 5b and c). Of note, *ABCA12* gene expression, as assessed by quantitative real-time reverse transcriptase-PCR, was elevated in organotypic skin equivalents downregulated for *CAPN12,* whereas protein expression was not significantly different (not shown). We considered the possibility that filaggrin deficiency in the patient skin may have been the result of biallelic mutations in the *FLG* gene. To rule out this possibility, the *FLG* gene was fully sequenced, which revealed no loss-of-function mutations (not shown). We also assessed the possibility that filaggrin deficiency may be related to ABCA12 dysfunction. However, as previously shown (Akiyama et al., 1996), we found normal to increased filaggrin expression in the skin of patients carrying biallelic null mutations in the *ABCA12* gene (Figure 5d). We also attempted to generate skin equivalents deficient for both calpain 12 and ABCA12, but were unable to obtain epidermal differentiation in these double knockdown skin models (not shown).

Second, we used *K14 H2B-GFP* mice to assess by ex vivo live imaging the effect of *Capn12* downregulation on hair cycling (Supplementary Fig. S7 online, Supplementary Movies S1–S3 online). As shown in Supplementary Figure S8 online, we achieved efficient downregulation of calpain 12 expression in skin strips derived from those mice. Live imaging revealed that calpain 12 downregulation induced catagen-like transformation in hair follicles (Figure 6). Many hair follicles treated with *Capn12* siRNA showed evidence of increased apoptotic activity (Supplementary Figure S9 online), suggesting that calpain 12 expression is essential for normal hair follicle cycling.

DISCUSSION

Disorders of cornification, and ARCI more specially, are known to be characterized by clinical heterogeneity (Oji et al., 2010), which in turn very much complicates both the diagnosis and the genetic counseling of families at risk for these disorders. Apart from the effect of filaggrin deficiency on the clinical manifestations of X-linked recessive ichthyosis (Liao et al., 2007) and pachyonychia congenita (Gruber et al., 2009), very little is currently known about genetic modifiers of clinical phenotypes in disorders of cornification. Here, we identified biallelic deleterious mutations in *CAPN12* in a child with exfoliative erythroderma carrying two mutations in *ABCA12*. Although congenital

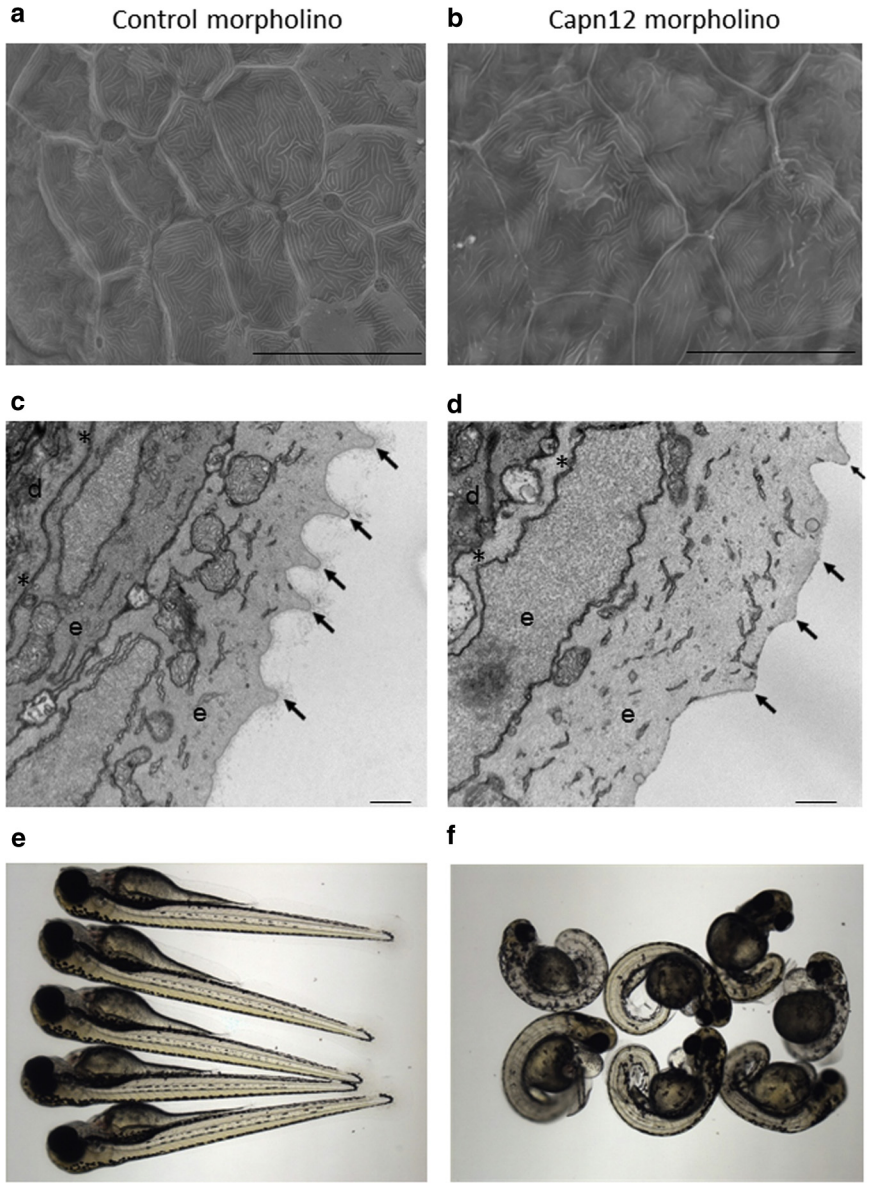

Figure 4. Capn12 knockdown in a zebrafish model. Zebrafish embryos were injected with a global standard control morpholino (scMO) (**a, c, e**) or with a *Capn12*-specific morpholino (**b, d, f**). Scanning electron microscopy analysis of the skin of the tail of a control larvae injected with scMO shows the presence of keratinocytes with well-demarcated cell−cell borders containing well-defined microridges (**a**), whereas the morphant larvae injected with a splice site morpholino for *Capn12* demonstrates perturbed microridge formation in the center of the keratinocytes with cracks and sloughing (**b**) (scale bar = 30 μm). Transmission electron microscopy analysis demonstrates normal microridge formation (arrows) in the control larva (**c**), whereas the formation of microridges in the morphant fish (**d**) is markedly perturbed (arrows). Asterisks mark the basement membrane. e, epidermis; d, dermis. Scale bar = 500 nm. In contrast with the normal morphology of the control fish (**e**), the morphant fish developed pericardial edema and a curled tail phenotype associated with death at around 6−8 days after fertilization (**f**).

erythroderma can be a consequence of mutations in *ABCA12*, several clinical (severe hypotrichosis and exuberant nail plate growth) and pathologic (loss of epidermal architecture and lack of hyperkeratosis) features were deemed atypical of ARCI. Severe alopecia has been reported in the context of harlequin ichthyosis, but ARCI is usually associated with no or a mild hair phenotype as previously shown in a patient carrying p.R986W and a splice site mutation (Fukuda et al., 2012).

Calpains form a large family of 14 distinct calcium-dependent cysteine proteinases that share a similar protease domain (Goll et al., 2003). They have been shown to regulate major cellular functions including apoptosis and cell motility and have been implicated in the pathogenesis of human diseases such as cancer, cardiovascular, and neurodegenerative disorders (Miyazaki et al., 2013; Momeni, 2011; Ono and Sorimachi, 2012; Sorimachi et al., 2012; Storr et al., 2011; Vosler et al., 2008). Several lines of evidence suggest that calpains may play an important role in cutaneous biology. Calpain inhibition was found to be associated with abnormal cornification (Kim and Bae, 1998) and delayed wound healing (Nassar et al., 2012), whereas calpain activity was also found to be necessary for staphylococci to break through the epidermal barrier (Soong et al., 2012). More recently, calpastin, a calpain inhibitor, was found to be absent in the skin of patients with PLACK syndrome (MIM 616295), which is characterized by peeling skin, leukonychia, acral keratosis, cheilitis, and keratoderma as well as by loss of epidermal cell-cell adhesion (Lin et al., 2015). Although most calpains are distributed ubiquitously, a minority of these proteinases are expressed in a tissue-specific fashion, including calpain 12, which is predominantly expressed in the skin (this study and Dear et al., 2000).

Here we show that calpain 12 plays a pivotal role in epidermal differentiation and hair follicle cycling. In agreement with our data, a recent paper identified capn12 as essential for skin integrity in zebrafish (Westcot et al., 2015). Although the exact mechanism underlying calpain 12 mode

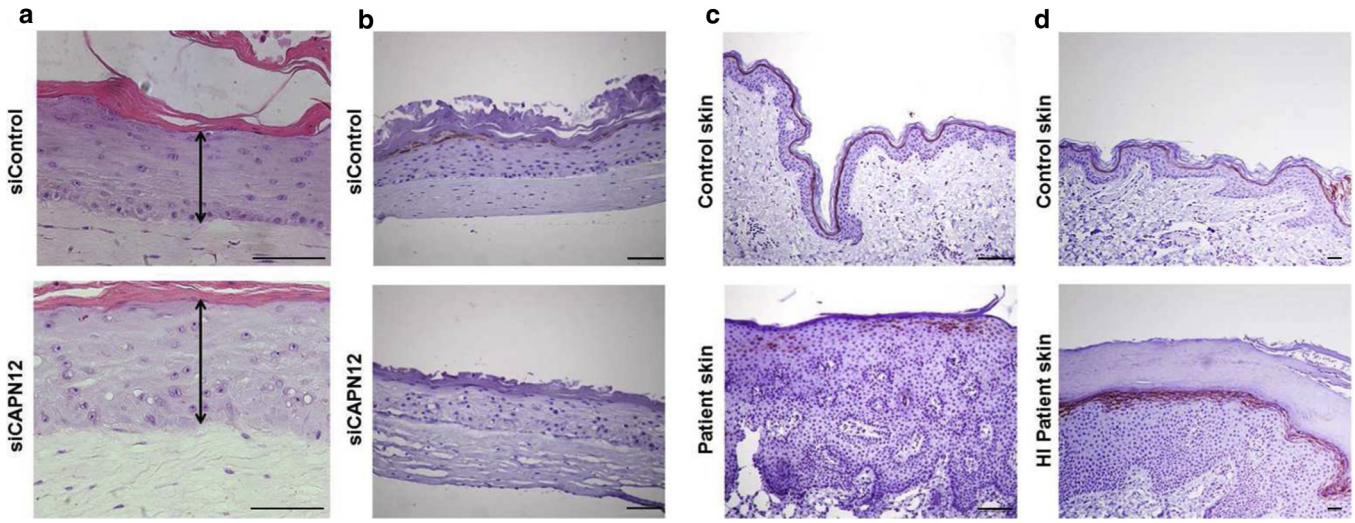

Figure 5. *CAPN12* knockdown in organotypic cell cultures. (**a, b**) Human primary keratinocytes transfected with *CAPN12* siRNA (siCAPN12) or control small interfering RNA (siControl) were used to generate skin equivalents. Punch biopsies were obtained from skin equivalents at day10 and stained for (**a**) hematoxylin and eosin or (**b**) filaggrin (scale bar = 100 μm). (**c**) Punch biopsies were obtained from control skin and from the patient (III-1) skin and stained for filaggrin (scale bar = 100 μm). (**d**) Punch biopsies were obtained from control skin and from the skin of a patient with harlequin ichthyosis and biallelic null mutations in the *ABCA12* gene and stained for filaggrin (scale bar = 100 μm).

of action during epidermal differentiation remains to be determined, the histopathologic findings secondary to CAPN12 downregulation in three-dimensional models suggest that calpain 12 deficiency may interfere with the normal processing and/or activation of critical components of the cornified cell envelope. This hypothesis is in line with earlier studies that suggested that calpains contribute to epidermal maturation by activating transglutaminase 1 and promoting the processing of filaggrin (Kim and Bae, 1998; Resing et al., 1993; Yamazaki et al., 1997). In fact, filaggrin expression was markedly reduced and mislocalized in the skin of the patient. The fact that downregulation of *CAPN12* in three-dimensional skin equivalents was also associated with filaggrin deficiency argues for a direct role of calpain 12 in the regulation of filaggrin expression in the differentiating epidermis. Filaggrin deficiency could in part underlie the unusual severity of this patient's condition as *FLG* mutations have been associated with both epidermal and follicular phenotypes (Meng et al., 2014), although it is possible that other abnormalities (e.g., abnormal expression of adhesion molecules, which are known to play an important role in the regulation of cornification; Harmon et al., 2013) are also responsible for the overall severe phenotype displayed by the patient.

Recently, another atypical case of ARCI caused by mutations in *NIPAL4* was also shown to be associated with modifying genetic variations in genes modulating epidermal differentiation (Kiritsi et al., 2015), substantiating the notion that the phenotypic variability typical of ARCI could often be attributable to minor genetic variants in genes encoding elements of the epidermal differentiation program.

In summary, we have shown that calpain 12 plays a crucial role in interfollicular and follicular epidermal differentiation. In addition, calpain 12 deficiency may modify the clinical consequences of *ABCA12* mutations, although its role as a genetic modifier remains to be confirmed in additional cases. Given initial studies showing the involvement of calpains in the pathogenesis of both inherited (Lin et al., 2015) and acquired (Gutowska-Owsiak et al., 2012; Meephansan et al., 2012) cutaneous disorders, the present observations warrant investigating calpain 12 as a potential therapeutic target for some of these conditions.

MATERIALS AND METHODS

Patients

All affected and healthy family members or their legal guardian provided written and informed consent according to a protocol approved by our institutional review board and by the Israel National Committee for Human Genetic Studies in adherence with the Helsinki principles.

Exome sequencing

Details regarding exome sequencing can be found in Supplementary Materials and Methods online.

Mutation analysis

Technical details regarding mutation analysis and direct sequencing can be found in Supplementary Materials and Methods.

PCR-restriction fragment length polymorphism

Technical details regarding the design and execution of these assays can be found in Supplementary Materials and Methods.

Bisulfite sequencing

Technical details regarding the design and execution of bisulfite sequencing can be found in Supplementary Materials and Methods.

Quantitative real-time reverse transcriptase-PCR

Technical details regarding quantitative real-time reverse transcriptase-PCR can be found in Supplementary Materials and Methods.

Cell cultures and reagents

Primary KCs and fibroblasts were isolated from adult skin obtained from plastic surgery specimens after having received written informed consent from the donors according to a protocol reviewed and approved by our institutional review board as previously described (Samuelov et al., 2013). Primary KCs were maintained in Keratinocytes Growth Medium (Lonza, Walkersville, MD).

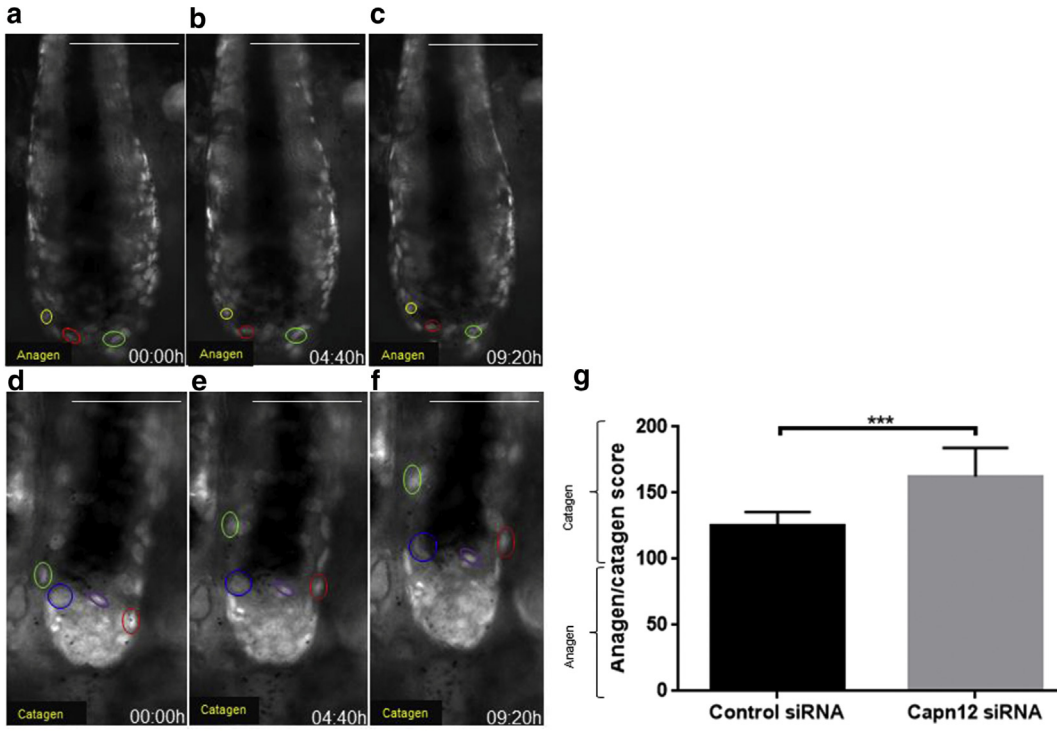

Figure 6. Effect of *Capn12* downregulation on the hair follicle cycle. (**a**–**f**) Z stacks optical sections of *K14-H2B-GFP* mouse anagen (**a**–**c**) and catagen (**d**–**f**) hair follicles treated with control small interfering RNA (siRNA) and *Capn12* siRNA, respectively. The anagen hair follicles show the stationary location of epithelial nuclei (see Supplementary Movie S1), whereas the catagen hair follicles demonstrate upward movement of the epithelial nuclei (see Supplementary Movie S3) during 9:20 hours of imaging. Epithelial nuclei are marked with K14-H2BGFP. Three nuclei in anagen (**a**–**c**) and four nuclei in catagen (**d**–**f**) hair follicles are circled in colors. Scale bar = 100 μm. (**g**) Anagen and catagen were ascertained as previously described (Foitzik et al., 2005; Samuelov et al., 2012). In brief, hair follicles were categorized as "alive" or "dead" based on the presence of any movement of cells in the follicle. "Alive" hair follicles were further categorized as anagen or catagen hair follicles based on the following defining parameters for catagen transformation: (1) hair bulb shrinkage and upward displacement of the bulb region, (2) upward displacement of epithelial nuclei in the bulb region, and (3) apoptosis of epithelial cells with evidence of nuclear fragmentation. Three independent experiments were performed with three different mice. In each mouse, three skin samples from each of the two treatment groups (*Capn12*-siRNA vs. control-siRNA) were used for ex vivo live imaging, and in each sample, the mean hair cycle score (HCS) was calculated as previously described (Foitzik et al., 2005; Samuelov et al., 2012). Results were pooled and are expressed as the mean HCS of all hair follicles per treatment group (***$P < 0.001$, *t*-test).

Fibroblasts were cultured in DMEM supplemented with 20% fetal calf serum (Biological Industries Israel, Beit-Haemek, Israel).

siRNA transfection

Primary KCs and fibroblasts were cultured in 100-mm culture plates at 37 °C in 5% CO_2 in a humidified incubator and were harvested at 60% confluence. To downregulate *CAPN12* expression, we used human *CAPN12* siRNA (Santa Cruz; sc-62060) (5′-GAACAG CGGAAUGAGUUCUtt-3′, 5′-CAAUCCUCAGUUCCGUUUAtt-3′, and 5′-CGUACUCCUCACUCAGAAAtt-3′). As control siRNA, we used Stealth RNAi Negative Control Duplex (Invitrogen, Carlsbad, CA). One hundred and eighty picomoles of siRNAs were transfected into primary KCs and fibroblasts using Lipofectamine RNAiMax (Invitrogen). The transfection medium was replaced after 6 hours with Keratinocytes Growth Medium (for KCs) or DMEM (for fibroblasts). Seventy-two hours after transfection, the transfected cells were trypsinized and used for organotypic cell cultures as described below.

Preparation of organotypic cell cultures

Experimental details regarding the generation of organotypic cell cultures can be found in Supplementary Materials and Methods.

Immunostaining

Details regarding immunostaining techniques can be found in Supplementary Materials and Methods.

Capn12 knockdown in zebrafish and morphant analysis

Details of the generation of capn12-deficient zebrafish embryos can be found in Supplementary Materials and Methods.

Ex vivo hair follicle live imaging

Details regarding the generation and use of *K14 H2B-GFP*$^{+/+}$ mice to ascertain the effect of Capn12 deficiency on hair follicle can be found in Supplementary Materials and Methods.

ORCID

W. H. Irwin McLean: http://orcid.org/0000-0001-5539-5757

CONFLICT OF INTEREST

The authors state no conflict of interest.

ACKNOWLEDGMENTS

This study was supported in part by a generous donation of the Ram family (ES), by the National Institutes of Health Support (CA) (5T32AR062496-03) and by a Wellcome Trust Strategic Award (098439/Z/12/Z to WHIM). We would like to thank Jennifer L. Koetsier, Robert M. Harmon, Nicole Najor, Lisa Godsel, and Kathleen J. Green (Department of Pathology, Northwestern University, Chicago, IL) for insightful discussions.

SUPPLEMENTARY MATERIAL

Supplementary material is linked to the online version of the paper at www.jidonline.org, and at http://dx.doi.org/10.1016/j.jid.2016.07.043.

REFERENCES

Adzhubei IA, Schmidt S, Peshkin L, Ramensky VE, Gerasimova A, Bork P, et al. A method and server for predicting damaging missense mutations. Nat Methods 2010;7:248–9.

Akiyama M, Yoneda K, Kim SY, Koyama H, Shimizu H. Cornified cell envelope proteins and keratins are normally distributed in harlequin ichthyosis. J Cutan Pathol 1996;23:571–5.

Berezin C, Glaser F, Rosenberg J, Paz I, Pupko T, Fariselli P, et al. ConSeq: the identification of functionally and structurally important residues in protein sequences. Bioinformatics 2004;20:1322–4.

Campbell RL, Davies PL. Structure-function relationships in calpains. Biochem J 2012;447:335–51.

Cooper DN, Krawczak M, Polychronakos C, Tyler-Smith C, Kehrer-Sawatzki H. Where genotype is not predictive of phenotype: towards an understanding of the molecular basis of reduced penetrance in human inherited disease. Hum Genet 2013;132:1077–130.

Dear TN, Meier NT, Hunn M, Boehm T. Gene structure, chromosomal localization, and expression pattern of Capn12, a new member of the calpain large subunit gene family. Genomics 2000;68:152–60.

Foitzik K, Spexard T, Nakamura M, Halsner U, Paus R. Towards dissecting the pathogenesis of retinoid-induced hair loss: all-trans retinoic acid induces premature hair follicle regression (catagen) by upregulation of transforming growth factor-beta2 in the dermal papilla. J Invest Dermatol 2005;124:1119–26.

Fukuda S, Hamada T, Ishii N, Sakaguchi S, Sakai K, Akiyama M, et al. Novel adenosine triphosphate (ATP)-binding cassette, subfamily A, member 12 (ABCA12) mutations associated with congenital ichthyosiform erythroderma. Br J Dermatol 2012;166:218–21.

Goll DE, Thompson VF, Li H, Wei W, Cong J. The calpain system. Physiol Rev 2003;83:731–801.

Gruber R, Wilson NJ, Smith FJ, Grabher D, Steinwender L, Fritsch PO, et al. Increased pachyonychia congenita severity in patients with concurrent keratin and filaggrin mutations. Br J Dermatol 2009;161:1391–5.

Gutierrez-Arcelus M, Ongen H, Lappalainen T, Montgomery SB, Buil A, Yurovsky A, et al. Tissue-specific effects of genetic and epigenetic variation on gene regulation and splicing. PLoS Genet 2015;11:e1004958.

Gutowska-Owsiak D, Schaupp AL, Salimi M, Selvakumar TA, McPherson T, Taylor S, et al. IL-17 downregulates filaggrin and affects keratinocyte expression of genes associated with cellular adhesion. Exp Dermatol 2012;21:104–10.

Harmon RM, Simpson CL, Johnson JL, Koetsier JL, Dubash AD, Najor NA, et al. Desmoglein-1/Erbin interaction suppresses ERK activation to support epidermal differentiation. J Clin Invest 2013;123:1556–70.

Isakov O, Perrone M, Shomron N. Exome sequencing analysis: a guide to disease variant detection. Methods Mol Biol 2013a;1038:137–58.

Isakov O, Rinella ES, Olchovsky D, Shimon I, Ostrer H, Shomron N, et al. Missense mutation in the MEN1 gene discovered through whole exome sequencing co-segregates with familial hyperparathyroidism. Genet Res (Camb) 2013b;95:114–20.

Kim SY, Bae CD. Calpain inhibitors reduce the cornified cell envelope formation by inhibiting proteolytic processing of transglutaminase 1. Exp Mol Med 1998;30:257–62.

Kiritsi D, Valari M, Fortugno P, Hausser I, Lykopoulou L, Zambruno G, et al. Whole-exome sequencing in patients with ichthyosis reveals modifiers associated with increased IgE levels and allergic sensitizations. J Allergy Clin Immunol 2015;135:280–3.

Kumar P, Henikoff S, Ng PC. Predicting the effects of coding non-synonymous variants on protein function using the SIFT algorithm. Nat Protoc 2009;4:1073–81.

Lev Maor G, Yearim A, Ast G. The alternative role of DNA methylation in splicing regulation. Trends Genet 2015;31:274–80.

Li Q, Uitto J. Zebrafish as a model system to study heritable skin diseases. Methods Mol Biol 2013;961:411–24.

Liao H, Waters AJ, Goudie DR, Aitken DA, Graham G, Smith FJ, et al. Filaggrin mutations are genetic modifying factors exacerbating X-linked ichthyosis. J Invest Dermatol 2007;127:2795–8.

Lin Z, Zhao J, Nitoiu D, Scott CA, Plagnol V, Smith FJ, et al. Loss-of-function mutations in CAST cause peeling skin, leukonychia, acral punctate keratoses, cheilitis, and knuckle pads. Am J Hum Genet 2015;96:440–7.

Malousi A, Kouidou S. DNA hypermethylation of alternatively spliced and repeat sequences in humans. Mol Genet Genomics 2012;287:631–42.

Maunakea AK, Chepelev I, Cui K, Zhao K. Intragenic DNA methylation modulates alternative splicing by recruiting MeCP2 to promote exon recognition. Cell Res 2013;23:1256–69.

Meephansan J, Tsuda H, Komine M, Tominaga S, Ohtsuki M. Regulation of IL-33 expression by IFN-gamma and tumor necrosis factor-alpha in normal human epidermal keratinocytes. J Invest Dermatol 2012;132:2593–600.

Meng L, Wang L, Tang H, Tang X, Jiang X, Zhao J, et al. Filaggrin gene mutation c.3321delA is associated with various clinical features of atopic dermatitis in the Chinese Han population. PLoS One 2014;9:e98235.

Miyazaki T, Koya T, Kigawa Y, Oguchi T, Lei XF, Kim-Kaneyama JR, et al. Calpain and atherosclerosis. J Atheroscler Thromb 2013;20:228–37.

Momeni HR. Role of calpain in apoptosis. Cell J 2011;13:65–72.

Nassar D, Letavernier E, Baud L, Aractingi S, Khosrotehrani K. Calpain activity is essential in skin wound healing and contributes to scar formation. PLoS One 2012;7:e37084.

Oji V, Tadini G, Akiyama M, Blanchet Bardon C, Bodemer C, Bourrat E, et al. Revised nomenclature and classification of inherited ichthyoses: results of the First Ichthyosis Consensus Conference in Soreze 2009. J Am Acad Dermatol 2010;63:607–41.

Ono Y, Sorimachi H. Calpains: an elaborate proteolytic system. Biochim Biophys Acta 2012;1824:224–36.

Pollard KS, Hubisz MJ, Rosenbloom KR, Siepel A. Detection of nonneutral substitution rates on mammalian phylogenies. Genome Res 2010;20:110–21.

Pruszkowski A, Bodemer C, Fraitag S, Teillac-Hamel D, Amoric JC, de Prost Y. Neonatal and infantile erythrodermas: a retrospective study of 51 patients. Arch Dermatol 2000;136:875–80.

Resing KA, al-Alawi N, Blomquist C, Fleckman P, Dale BA. Independent regulation of two cytoplasmic processing stages of the intermediate filament-associated protein filaggrin and role of Ca^{2+} in the second stage. J Biol Chem 1993;268:25139–45.

Samuelov L, Sarig O, Harmon RM, Rapaport D, Ishida-Yamamoto A, Isakov O, et al. Desmoglein 1 deficiency results in severe dermatitis, multiple allergies and metabolic wasting. Nat Genet 2013;45:1244–8.

Samuelov L, Sprecher E. Peeling off the genetics of atopic dermatitis-like congenital disorders. J Allergy Clin Immunol 2014;134:808–15.

Samuelov L, Sprecher E, Tsuruta D, Biro T, Kloepper JE, Paus R. P-cadherin regulates human hair growth and cycling via canonical Wnt signaling and transforming growth factor-beta2. J Invest Dermatol 2012;132:2332–41.

Siepel A, Bejerano G, Pedersen JS, Hinrichs AS, Hou M, Rosenbloom K, et al. Evolutionarily conserved elements in vertebrate, insect, worm, and yeast genomes. Genome Res 2005;15:1034–50.

Siepel A, Pollard K, Haussler D. New methods for detecting lineage-specific selection. In: Apostolico A, Guerra C, Istrail S, Pevzner P, Waterman M, editors. Research in computational molecular biology. Berlin, Heidelberg: Springer; 2006. p. 190–205.

Soong G, Chun J, Parker D, Prince A. Staphylococcus aureus activation of caspase 1/calpain signaling mediates invasion through human keratinocytes. J Infect Dis 2012;205:1571–9.

Sorimachi H, Mamitsuka H, Ono Y. Understanding the substrate specificity of conventional calpains. Biol Chem 2012;393:853–71.

Storr SJ, Carragher NO, Frame MC, Parr T, Martin SG. The calpain system and cancer. Nat Rev Cancer 2011;11:364–74.

Vosler PS, Brennan CS, Chen J. Calpain-mediated signaling mechanisms in neuronal injury and neurodegeneration. Mol Neurobiol 2008;38:78–100.

Westcot SE, Hatzold J, Urban MD, Richetti SK, Skuster KJ, Harm RM, et al. Protein-trap insertional mutagenesis uncovers new genes involved in zebrafish skin development, including a neuregulin 2a-based ErbB signaling pathway required during median fin fold morphogenesis. PLoS One 2015;10:e0130688.

Yamazaki M, Ishidoh K, Suga Y, Saido TC, Kawashima S, Suzuki K, et al. Cytoplasmic processing of human profilaggrin by active mu-calpain. Biochem Biophys Res Commun 1997;235:652–6.